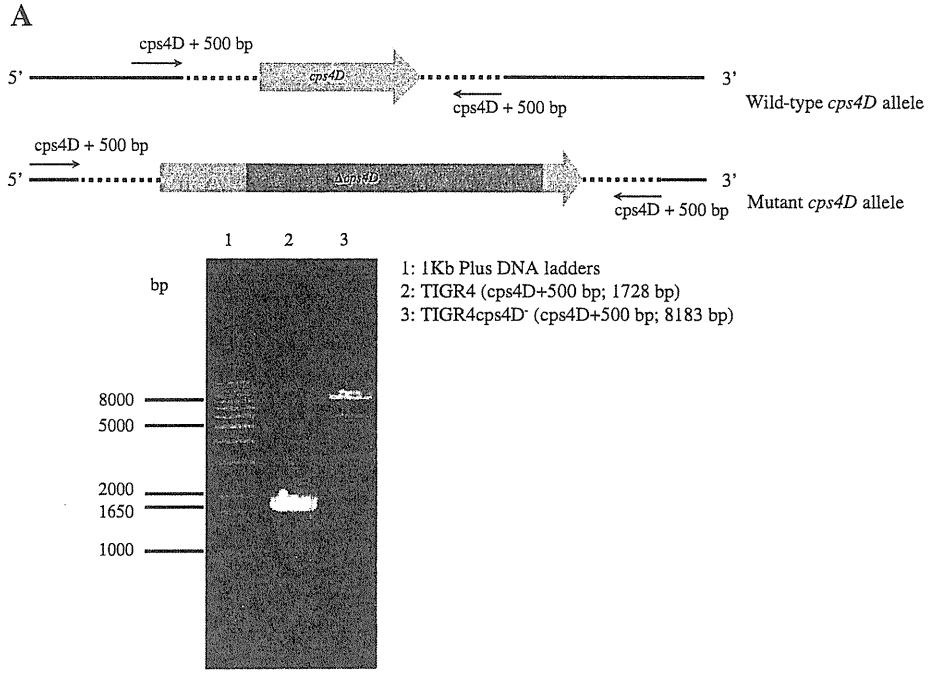

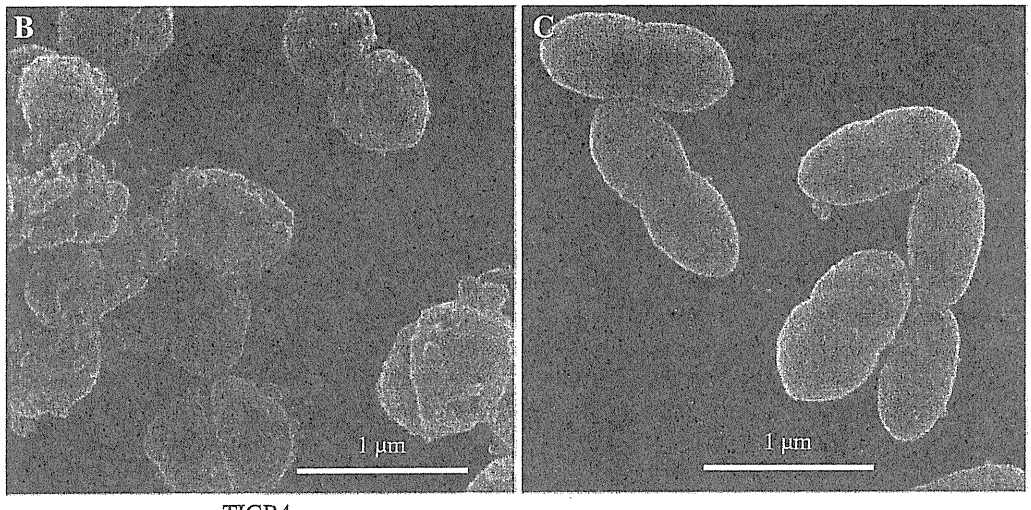

TIGR4 TIGR4cps4D-

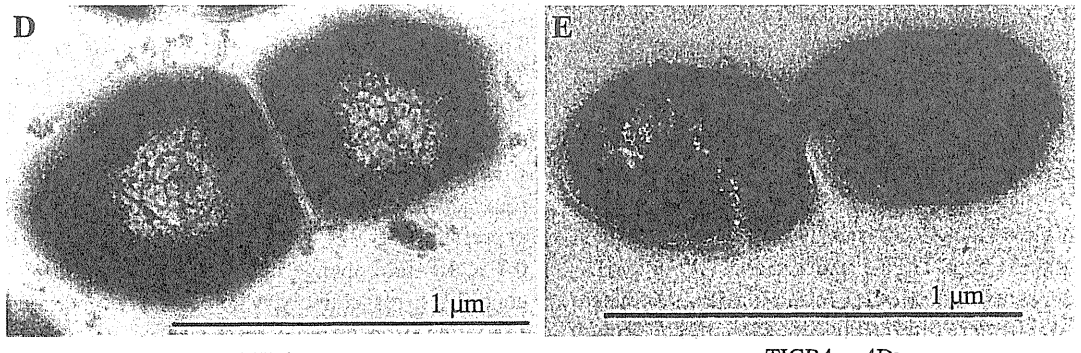

TIGR4 TIGR4cps4D-

◀ **Fig. 1** **a** Confirmation of the mutant by polymerase chain reaction (PCR). Primers were designed to span a region 500 bp up- and downstream from the *cps4D* gene for confirmation of the capsular polysaccharide-impaired mutant. **b**, **c** Capsular polysaccharide (CPS) on the cell surface of TIGR4 and TIGR4cps4D$^-$ observed by scanning electron microscopy (SEM). A representative bacterium is shown for TIGR4 and TIGR4cps4D$^-$, respectively. **d**, **e** CPS on the cell surface of TIGR4 and TIGR4cps4D$^-$ observed by transmission electron microscopy (TEM). A representative bacterium is shown for TIGR4 and TIGR4cps4D$^-$, respectively. **b**, **c**, **d**, **e** ×30,000

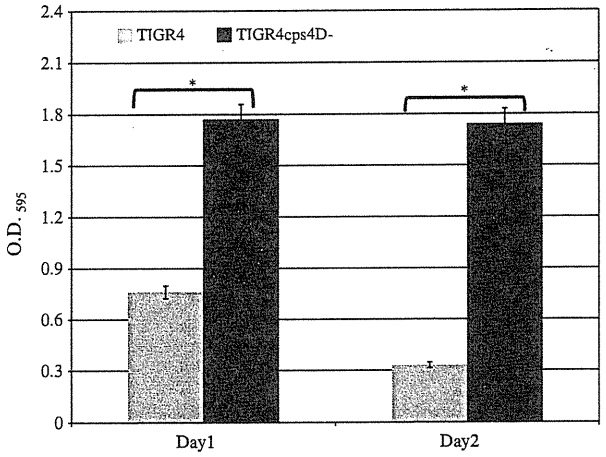

Strains growth (OD_{490})	TIGR4	TIGR4cps4D$^-$	P values
Day 1	0.23 ±0.04	0.18 ±0.01	P= 0.375
Day 2	0.24 ±0.02	0.13 ±0.01	P= 0.001

Fig. 2 Biofilm formation capacity of TIGR4 and TIGR4cps4D$^-$. Bacterial cells were cultured in BHI broth at 37 °C for 24 and 48 h, and the growths were investigated before assay. *Gray and black bars* indicate the biofilm formation of TIGR4 and TIGR4cps4D$^-$, respectively. Results are average ± SD of three independent experiments. *$P < 0.0001$

4.9×10^2-, 2.4×10^3-, 3.2×10^1-, 4.7×10^2-, and 3.6×10^1-fold higher compared to TIGR4, except the expressions of *lytA* and *IgA1*, which were 1.9×10^{-5}- and 9.7×10^{-5}-fold lower, respectively (Fig. 4b).

Pathogenic effect of TIGR4cps4D$^-$ infection on viability of BEAS-2B cells

To ensure the pathogenicity of the TIGR4cps4D$^-$ strain in our experiments, a cytotoxicity detection assay was performed. BEAS-2B cell death was evaluated by LDH release, following an infection with TIGR4 and TIGR4cps4D$^-$ after an incubation of 5 or 24 h (Fig. 5). TIGR4 increased cell death from 33.47 to 45.41 %, and TIGR4cps4D$^-$ also increased cell death from 21.38 to 31.44 %, after 5 and 24 h exposure, respectively. The figure reveals that TIGR4cps4D$^-$ significantly reduced BEAS-2B cell death compared to TIGR4, when observed after 5 or 24 h exposure ($P < 0.05$).

Discussion

In this study we observed mature biofilms produced by both TIGR4 and its CPS-impaired mutant TIGR4cps4D$^-$. These data provide direct evidence that *S. pneumoniae* forms mature biofilms in vitro. Furthermore, because TIGR4cps4D$^-$ formed a larger and thicker biofilm than did its parental strain, loss of CPS has the potential to promote biofilm formation (or possibly quicken the biofilm formation in the early adherence). Previous studies reported that a series of derivatives from the clinical or laboratory-originated pneumococcal isolates expressed comparable amounts of CPS that differed from that of the parental strain, and some of these CPS exhibited reduced biofilm formation [6]. These results indicate that CPS is actually involved in biofilm formation. In our study, electron microscopy confirmed the disruption of CPS secretion, which subsequently promoted biofilm formation. This interesting finding gives the direct evidence to reveal the relatedness of CPS expression and pneumococcal biofilm formation. CPS was reported to block the function of a self-recognizing adhesin 43 through physical shielding and sterically prevent receptor–target recognition of short bacterial adhesins, and this negative interference affects the ability of bacteria adherence during the initial colonization phase.

psaA encodes a surface-exposed common 37-kDa multifunctional lipoprotein detected on all known serotypes of *S. pneumoniae*. It also plays a major role in pneumococcal attachment to the host cell and virulence [34]. In our study, alternating expression was detected for *psaA* under planktonic conditions and biofilms. The higher expression level of *psaA* in TIGR4cps4D$^-$ in biofilms indicated that impaired CPS might influence *psaA* expression, but this should be tested by further similar experiments with the addition of exogenous CPS to non-CPS-expressing TIGR4cps4D$^-$ or co-culture with other bacterial species that produce biofilms. Our results indicated that the TIGR4 strain formed fewer biofilms than did the CPS-impaired mutant, which may be caused by either sterical shielding of adhesion proteins by the CPS or CPS production interfering with synthesis or transport of adhesion proteins to the cell surface, as Schembri et al. [35] demonstrated.

In the previous studies, biofilms were most often grown in Todd–Hewitt broth [6, 8–10] whereas very few studies used BHI broth as the culture medium. In our studies, mature biofilms were observed after 24 or 48 h of continuous culture in BHI broth, which proved that BHI is also suitable for biofilm study. Although in biofilms the gene expression of *lytA* in TIGR4cps4D$^-$ was 1.9×10^{-5}-fold lower than TIGR4, we noticed that the number of dead pneumococcal cells was increased in the TIGR4cps4D$^-$ biofilms (Fig. 3b). The reason remains unclear; the

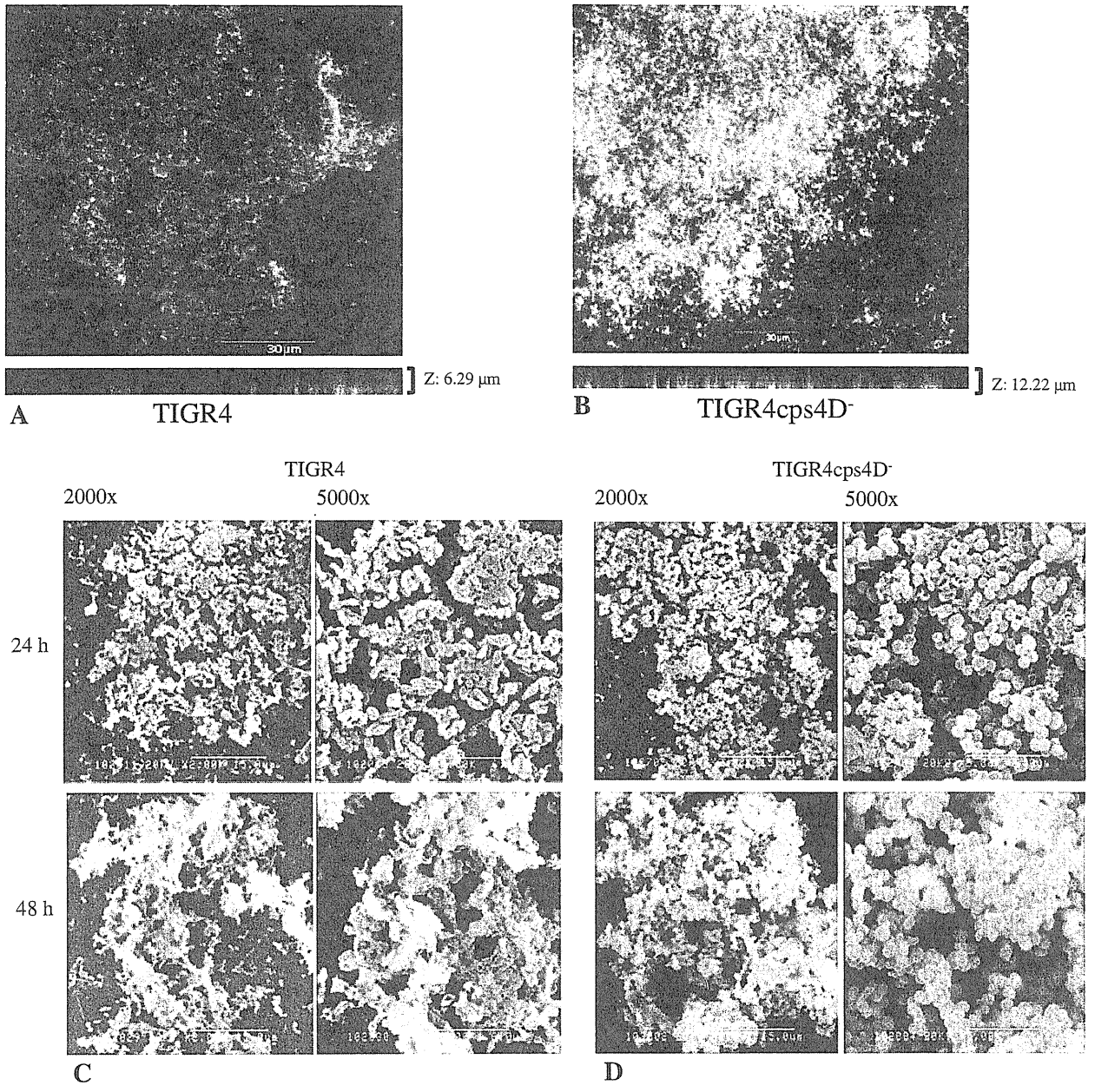

Fig. 3 Biofilm architecture with confocal laser scanning microscopy (CLSM) and SEM visually observed after 24 h of culture. CLSM images (**a**, **b**) show the *x*–*y* and *x*–*z* planes. Flow-cell experiments were performed in triplicate as described in "Materials and methods." *Bars* 30 μm. ×400. Biofilm architecture visually observed with SEM (**c**, **d**) after 24 and 48 h of culture, respectively; SEM images were taken at 2,000× and 5,000× for each strain

effective inhibition of pneumococcal autolysin is thought to be a priority of future pneumococcal biofilm studies. Allegrucci and Sauer [9] reported the biofilm development process occurred in three distinct stages, and biofilm viable cell counts and total protein concentration increased steadily over the course of biofilm development, reaching $\sim 8 \times 10^8$ cells and ~ 15 mg protein per biofilm after 9 days of biofilm growth. However, another study [7] reported that the total biofilm cell counts stabilized after 21 h, at approximately 10^5 cells/cm^2, whereas viable counts decreased as the biofilm aged. Thus, we think it should not be easy to judge whether pneumococcal biofilms detach after a longer period of time. As the biofilm seemed to be affected by many factors such as culture condition, medium, and strains, more studies should be focused on this aspect.

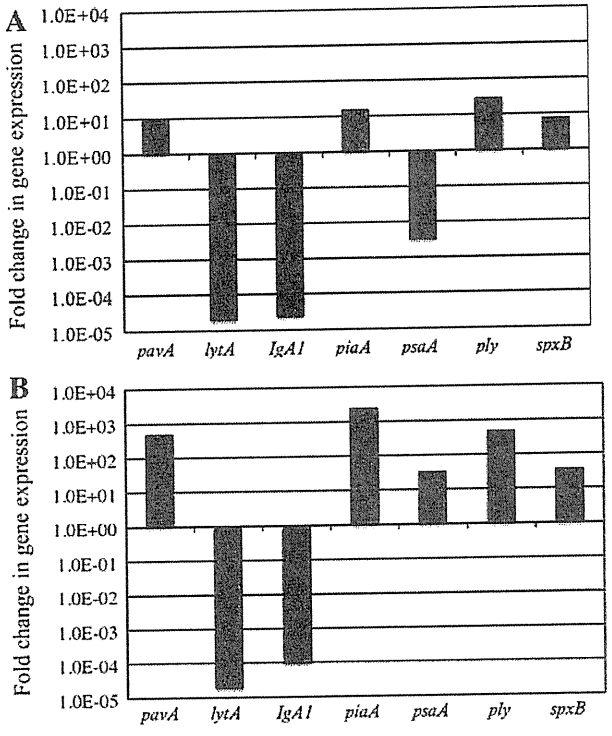

Fig. 4 Expression level of genes relative to adherence or virulence in TIGR4cps4D$^-$ compared to TIGR4. Strains were grown in BHI broth (**a**) to the stationary phase, and total RNA was analyzed by real-time PCR analysis using primers specific for *pavA*, *lytA*, *IgA1*, *piaA*, *psaA*, *ply*, and *spxB*. Gene expression of RNA isolated from biofilms (**b**) was analyzed

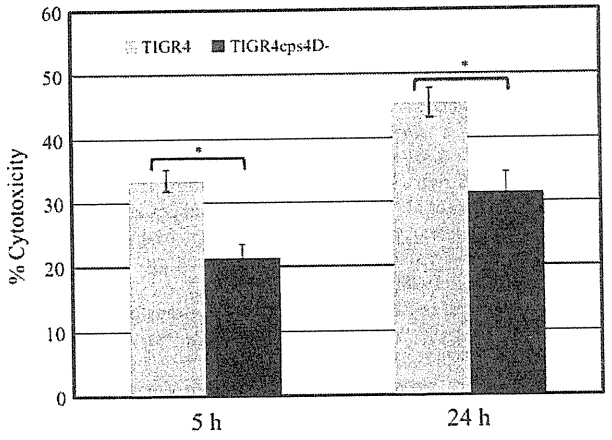

Fig. 5 BEAS-2B cells were assessed for cytotoxicity following an infection with TIGR4 and TIGR4cps4D$^-$ strains. Cytotoxicity was quantitated based on the measurement of LDH activity released from damaged cells after 5 and 24 h culture, respectively. Results are average ± SD of three independent experiments. $^*P < 0.05$

S. pneumoniae is capable of producing CPS, which is structurally distinct for each of 90 known serotypes and is essential for pneumococcal virulence [15, 36]. Maximal expression of CPS is essential for systemic virulence because of its antiphagocytic properties. A previous study reported that a *cps2D*-deleted D39 strain that produced a reduced amount of CPS was avirulent [37]. In the present study, the CPS-impaired mutant seemed to be reduced in pathogenicity compared to its parental strain. We also investigated the expression of seven genes based on their putative functions relative to adherence and virulence. *lytA* encoded autolysin, which may play a direct role in virulence by mediating the release of cell-wall components shown to be highly inflammatory, and in pathogenesis by mediating cell lysis and the subsequent release of virulence factors, such as pneumolysin. As a result, much higher expressions were detected for *lytA* and *IgA1* in TIGR4 under both planktonic conditions and biofilms. Previous studies found that disruption of the gene encoding the autolysin LytA reduces competence-induced cell lysis two- to fourfold [38], and interruption of the chromosomal gene resulted in loss of expression of an approximately 200-kDa protein and complete elimination of detectable IgA1 protease activity [39]. These results suggested that the interrupted *lytA* and *IgA1* expression might be responsible for the reduced pathogenicity of TIGR4cps4D$^-$. As is well known, pneumolysin was reported as an important virulence factor, contributing to multiple stages of the pathogenic process, and it is also involved in eliciting an immune response from the host. The cytotoxic characteristic of pneumolysin facilitates progression of diseases by inhibiting ciliary beating in the human respiratory epithelium, and also acts by disrupting tight junctions between epithelial cells. Additionally, numerous studies demonstrated that mutants lacking pneumolysin showing reduced replication and survival in the bloodstream of infected animals [40, 41]. Higher expression was detected for *ply* in TIGR4cps4D$^-$, with reduced cytotoxicity. Because pneumolysin production is regulated at a posttranscriptional level, it may be regulated independently of environmental stimuli, with the niche influencing the release of the toxin rather than its transcription or translation, as suggested by LeMessurier et al. [22]. There are some limitations of the present study. We hypothesize the CPS product, expressions of *pavA*, *lytA*, *IgA1*, *piaA*, *psaA*, *ply*, and *spxB*, played the important role in inducing cytotoxicity, but we did not investigate the protein/transcriptional levels of pneumolysin, as well as the other genes; thus, we could not demonstrate the key factor expressing cytotoxicity in this experiment or how impaired CPS affects the expression of virulence genes. Furthermore, whether TIGR4cps4D$^-$ was able to reduce pathogenicity after adherence to epithelial cells or tissues, and then formed mature biofilms by avoiding the clearance of host immune responses, has not been investigated. Thus, an animal model is thought to be necessary for future work.

The biofilm matrix was reported to be regulated by CPS, protein components, and other extracellular molecules. Pneumococci with different serotypes have different surface properties that may promote (or hinder) biofilm formation and may be very important for the survival of pneumococci in different host environments. Hammerschmidt et al. [42] found invasive pneumococci exhibited an enhanced capacity to adhere and invade epithelial cells, appearing to cause a reduction in capsular material, which potentially increases biofilm formation. If invasive pneumococci acquire enhanced ability to form biofilms, their elimination would become difficult, with subsequent serious clinical implications. Variations in CPS may result in different biofilm phenotypes. Therefore, screening of strains that form biofilms with vaccine serotypes is important not only for development of new vaccine candidates but for reevaluation of existing pneumococcal vaccines, e.g., a 23-valent polysaccharide vaccine, or a 7-valent conjugated vaccine.

The present study demonstrated that CPS as a surface structure seems to be essential for regulation of biofilm development and virulence. The artificial disruption of CPS that increased biofilm formation may be caused by interference with the initial process of attachment in pneumococcus and subsequent biofilm development.

Acknowledgments We greatly appreciate the help of Mr. Ryuhei Higashi in the completion of the electron microscopy study. This study was funded by Health, Labour and Welfare Sciences Research Grants for Research on Emerging and Re-emerging Infectious Diseases (H20 shinko ippan 012) from the Japanese government.

Conflict of interest We declare that none of the authors has financial arrangements with any company whose product is mentioned prominently in this manuscript nor with any company making a competing product.

References

1. Fang GD, Fine M, Orloff J, Arisumi D, Yu VL, Kapoor W, et al. New and emerging etiologies for community-acquired pneumonia with implications for therapy. A prospective multicenter study of 359 cases. Medicine (Baltim). 1990;69:307–16.
2. Appelbaum PC. Antimicrobial resistance in *Streptococcus pneumoniae*: an overview. Clin Infect Dis. 1992;15:77–83.
3. Linares J, Pallares R, Alonso T, Perez JL, Ayats J, Gudiol F, et al. Trends in antimicrobial resistance of clinical isolates of *Streptococcus pneumoniae* in Bellvitge Hospital, Barcelona, Spain (1979–1990). Clin Infect Dis. 1992;15:99–105.
4. Rello J, Rodriguez R, Jubert P, Alvarez B. Severe community-acquired pneumonia in the elderly: epidemiology and prognosis. Study Group for Severe Community-Acquired Pneumonia. Clin Infect Dis. 1996;23:723–8.
5. Restrepo MI, Jorgensen JH, Mortensen EM, Anzueto A. Severe community-acquired pneumonia: current outcomes, epidemiology, etiology, and therapy. Curr Opin Infect Dis. 2001;14:703–9.
6. Moscoso M, Garcia E, Lopez R. Biofilm formation by *Streptococcus pneumoniae*: role of choline, extracellular DNA, and capsular polysaccharide in microbial accretion. J Bacteriol. 2006;188:7785–95.
7. Donlan RM, Piede JA, Heyes CD, Sanii L, Murga R, Edmonds P, et al. Model system for growing and quantifying *Streptococcus pneumoniae* biofilms in situ and in real time. Appl Environ Microbiol. 2004;70:4980–8.
8. Allegrucci M, Hu FZ, Shen K, Hayes J, Ehrlich GD, Post JC, et al. Phenotypic characterization of *Streptococcus pneumoniae* biofilm development. J Bacteriol. 2006;188:2325–35.
9. Allegrucci M, Sauer K. Characterization of colony morphology variants isolated from *Streptococcus pneumoniae* biofilms. J Bacteriol. 2007;189:2030–8.
10. McEllistrem MC, Ransford JV, Khan SA. Characterization of in vitro biofilm-associated pneumococcal phase variants of a clinically relevant serotype 3 clone. J Clin Microbiol. 2007; 45:97–101.
11. Costerton JW, Stewart PS, Greenberg EP. Bacterial biofilms: a common cause of persistent infections. Science. 1999;284: 1318–22.
12. Wolcott RD, Ehrlich GD. Biofilms and chronic infections. JAMA. 2008;299:2682–4.
13. Kolkman MA, van der Zeijst BA, Nuijten PJ. Diversity of capsular polysaccharide synthesis gene clusters in *Streptococcus pneumoniae*. J Biochem (Tokyo). 1998;123:937–45.
14. Garcia E, Llull D, Munoz R, Mollerach M, Lopez R. Current trends in capsular polysaccharide biosynthesis of *Streptococcus pneumoniae*. Res Microbiol. 2000;151:429–35.
15. Bentley SD, Aanensen DM, Mavroidi A, Saunders D, Rabbinowitsch E, Collins M, et al. Genetic analysis of the capsular biosynthetic locus from all 90 pneumococcal serotypes. PLoS Genet. 2006;2:e31.
16. Morona JK, Paton JC, Miller DC, Morona R. Tyrosine phosphorylation of CpsD negatively regulates capsular polysaccharide biosynthesis in *Streptococcus pneumoniae*. Mol Microbiol. 2000;35:1431–42.
17. Morona JK, Morona R, Miller DC, Paton JC. Mutational analysis of the carboxy-terminal (YGX)4 repeat domain of CpsD, an autophosphorylating tyrosine kinase required for capsule biosynthesis in *Streptococcus pneumoniae*. J Bacteriol. 2003;185: 3009–19.
18. Jiang SM, Wang L, Reeves PR. Molecular characterization of *Streptococcus pneumoniae* type 4, 6B, 8, and 18C capsular polysaccharide gene clusters. Infect Immun. 2001;69:1244–55.
19. Coffey TJ, Enright MC, Daniels M, Morona JK, Morona R, Hryniewicz W, et al. Recombinational exchanges at the capsular polysaccharide biosynthetic locus lead to frequent serotype changes among natural isolates of *Streptococcus pneumoniae*. Mol Microbiol. 1998;27:73–83.
20. Nesin M, Ramirez M, Tomasz A. Capsular transformation of a multidrug-resistant *Streptococcus pneumoniae* in vivo. J Infect Dis. 1998;177:707–13.
21. Tomasz A. New faces of an old pathogen: emergence and spread of multidrug-resistant *Streptococcus pneumoniae*. Am J Med. 1999;107:55S–62S.
22. LeMessurier KS, Ogunniyi AD, Paton JC. Differential expression of key pneumococcal virulence genes in vivo. Microbiology. 2006;152:305–11.
23. Mortier-Barriere I, de Saizieu A, Claverys JP, Martin B. Competence-specific induction of recA is required for full recombination proficiency during transformation in *Streptococcus pneumoniae*. Mol Microbiol. 1998;27:159–70.
24. Weiser JN, Bae D, Fasching C, Scamurra RW, Ratner AJ, Janoff EN. Antibody-enhanced pneumococcal adherence requires IgA1 protease. Proc Natl Acad Sci USA. 2003;100:4215–20.

25. Tettelin H, Nelson KE, Paulsen IT, Eisen JA, Read TD, Peterson S, et al. Complete genome sequence of a virulent isolate of Streptococcus pneumoniae. Science. 2001;293:498–506.
26. Mayer MP. A new set of useful cloning and expression vectors derived from pBlueScript. Gene (Amst). 1995;163:41–6.
27. Qin L, Watanabe H, Yoshimine H, Guio H, Watanabe K, Kawakami K, et al. Antimicrobial susceptibility and serotype distribution of *Streptococcus pneumoniae* isolated from patients with community-acquired pneumonia and molecular analysis of multidrug-resistant serotype 19F and 23F strains in Japan. Epidemiol Infect. 2006;134:1188–94.
28. Yother J, McDaniel LS, Briles DE. Transformation of encapsulated *Streptococcus pneumoniae*. J Bacteriol. 1986;168:1463–5.
29. Berry AM, Yother J, Briles DE, Hansman D, Paton JC. Reduced virulence of a defined pneumolysin-negative mutant of *Streptococcus pneumoniae*. Infect Immun. 1989;57:2037–42.
30. Inokuchi T, Yokoyama R, Higashi R, Takahashi Y, Miyajima S. Ultrastructure of the perineurial cell of the sciatic nerve in rats—a transmission and scanning electron microscopic study. Kurume Med J. 1991;38:221–32.
31. Kaji C, Watanabe K, Apicella MA, Watanabe H. Antimicrobial effect of fluoroquinolones for the eradication of nontypeable *Haemophilus influenzae* isolates within biofilms. Tohoku J Exp Med. 2008;214:121–8.
32. Davies DG, Parsek MR, Pearson JP, Iglewski BH, Costerton JW, Greenberg EP. The involvement of cell-to-cell signals in the development of a bacterial biofilm. Science. 1998;280:295–8.
33. Livak KJ, Schmittgen TD. Analysis of relative gene expression data using real-time quantitative PCR and the 2(-Delta Delta C(T)) method. Methods. 2001;25:402–8.
34. Rajam G, Anderton JM, Carlone GM, Sampson JS, Ades EW. Pneumococcal surface adhesin A (PsaA): a review. Crit Rev Microbiol. 2008;34:163–73.
35. Schembri MA, Dalsgaard D, Klemm P. Capsule shields the function of short bacterial adhesins. J Bacteriol. 2004;186:1249–57.
36. Martens P, Worm SW, Lundgren B, Konradsen HB, Benfield T. Serotype-specific mortality from invasive *Streptococcus pneumoniae* disease revisited. BMC Infect Dis. 2004;4:21.
37. Morona JK, Miller DC, Morona R, Paton JC. The effect that mutations in the conserved capsular polysaccharide biosynthesis genes *cpsA*, *cpsB*, and *cpsD* have on virulence of *Streptococcus pneumoniae*. J Infect Dis. 2004;189:1905–13.
38. Kausmally L, Johnsborg O, Lunde M, Knutsen E, Havarstein LS. Choline-binding protein D (CbpD) in *Streptococcus pneumoniae* is essential for competence-induced cell lysis. J Bacteriol. 2005;187:4338–45.
39. Wani JH, Gilbert JV, Plaut AG, Weiser JN. Identification, cloning, and sequencing of the immunoglobulin A1 protease gene of *Streptococcus pneumoniae*. Infect Immun. 1996;64:3967–74.
40. Boulnois GJ, Paton JC, Mitchell TJ, Andrew PW. Structure and function of pneumolysin, the multifunctional, thiol-activated toxin of *Streptococcus pneumoniae*. Mol Microbiol. 1991;5:2611–6.
41. Steinfort C, Wilson R, Mitchell T, Feldman C, Rutman A, Todd H, et al. Effect of *Streptococcus pneumoniae* on human respiratory epithelium in vitro. Infect Immun. 1989;57:2006–13.
42. Hammerschmidt S, Wolff S, Hocke A, Rosseau S, Muller E, Rohde M. Illustration of pneumococcal polysaccharide capsule during adherence and invasion of epithelial cells. Infect Immun. 2005;73:4653–67.

J Infect Chemother (2012) 18:865–871
DOI 10.1007/s10156-012-0429-0

ORIGINAL ARTICLE

Intrahost emergent dynamics of oseltamivir-resistant virus of pandemic influenza A (H1N1) 2009 in a fatally immunocompromised patient

Nobuyuki Hamada · Yutaka Imamura · Koyu Hara · Takahito Kashiwagi · Yoshihiro Imamura · Yoko Nakazono · Katsumi Chijiwa · Hiroshi Watanabe

Received: 30 January 2012 / Accepted: 30 April 2012 / Published online: 2 June 2012

Abstract The oseltamivir-resistant pandemic influenza virus A (2009 H1N1) with H275Y mutation in neuraminidase (NA) has been sporadically reported, and its wide spread remains a potential threat. Here we detected the uneven distribution of H275Y mutant virus in a patient who received a 21-day long-term administration of oseltamivir. Intrahost variation of the virus showed that the H275Y mutant virus was the predominant population in both nasopharynx and right lung, whereas the oseltamivir-sensitive virus comprised half the population in the left lung. By constructing minimum spanning trees, it is proposed that the H275Y mutant might be generated primarily in the nasopharynx, then spread to the right and left lungs.

Keywords Pandemic influenza A virus (H1N1) 2009 · Oseltamivir resistance · Quasi-species · Minimum spanning tree

Introduction

In March 2009, a new swine-origin influenza A (H1N1) virus (S-OIV) emerged first in Mexico and spread next to the United States [1]. Within a half-year, S-OIV expanded worldwide. Fortunately, most S-OIV was susceptible to oseltamivir, which is an effective anti-influenza drug, although most seasonal influenza A (H1N1) viruses had already developed resistance to this drug [2]. However, an oseltamivir-resistant pandemic influenza virus has rarely appeared in patients [3], even those who were under intensive care. To determine the appropriate antiviral treatment and eventually control the outbreak, it is important to elucidate the mechanism by which the oseltamivir-resistant influenza virus appears, as well as to monitor the antiviral susceptibility profile of that influenza virus.

Although molecular investigation of S-OIV was extensively performed worldwide, the evolutional dynamics of this virus in a single patient, especially in connection with oseltamivir resistance, were not yet elucidated [4]. In this report, we investigated that the dynamics of these influenza viruses in a single patient, and we discuss the mechanisms by which mutant clones appeared.

Materials and methods

The data were analyzed anonymously, and all clinical investigations have been conducted according to the principles expressed in the Declaration of Helsinki. Furthermore, this study (Number 11162) was approved by The Ethical Committee of Kurume University.

Patients and specimen collection

Case 1

On December 23, 2009 (day 1; Table 1), a 56-year-old man with multiple myeloma (IgA kappa) complained of fever

N. Hamada (✉) · K. Hara · T. Kashiwagi · Y. Imamura · Y. Nakazono · H. Watanabe
Division of Infectious Disease, Department of Infectious Medicine, Kurume University School of Medicine, 67 Asahimachi, Kurume 830-0011, Japan
e-mail: nhamada@med.kurume-u.ac.jp

Y. Imamura
Division of Hematology, St. Mary's Hospital, 422 Tsubukuhonmachi, Kurume 830-8543, Japan

K. Chijiwa
Fukuoka Institute of Health and Environmental Sciences, Fukuoka 818-0135, Japan

Table 1 Clinical examination and treatment of patients infected with 2009 H1N1 influenza virus

Case	Age, sex	Underlying disease	Days (h) after the onset	Specimen taken	Influenza diagnosis		Treatment	Outcome
					Rapid test	RT-PCR (virus population)		
1	56, male	Multiple myeloma	2	Nasopharyngeal	+	nt	Day 2–22: oseltamivir (75 mg twice daily)	Died on day 27
			8	Nasopharyngeal	+	nt		
			13	Nasopharyngeal	+	+ (100 % H275Y)		
			20	Nasopharyngeal	−	nt		
			22	Nasopharyngeal	+	nt		
			27	Nasopharyngeal	nt	−	Day 23: zanamivir (10 mg twice daily)	
				Right lung	nt	+ (100 % H275Y)		
				Left lung	nt	+ (25 % H275Y)		
2	66, female	Asthma COPD	4	Nasopharyngeal	+	+ (100 % wild type)	Day 1–7: oseltamivir	Died on day 9
3	20, female	None	1 (12 h)	Nasopharyngeal	+	+ (100 % wild type)	Day 1–5: oseltamivir	Recovered
4	9, female	None	1 (1 h, 24 h)	Nasopharyngeal	−, +	+ (100 % wild type)	Day 1–5: zanamivir	Recovered

(37.8 °C) and cough. A nasopharyngeal swab specimen was positive for influenza virus type A by the rapid diagnosis kit (Esplein Influenza A&B–N; Fujirebio, Tokyo, Japan) on day 2. Oseltamivir was administered on day 2. Administration was then maintained for 21 days, until January 13, 2009, because of prolonged disease. Methylprednisolone pulse therapy was initiated on day 2 for the treatment of acute respiratory distress syndrome (ARDS). On day 6, a chest radiograph showed an interstitial pattern in both lungs. The patient was intermittently placed on noninvasive positive pressure ventilation (NIPPV). On day 20 the patient improved, and a rapid test for influenza virus A showed negative. On day 22, the patient exhibited a positive cytomegalovirus (CMV)-antigenemia (more than 53 cells) as well as being positive for influenza A rapid test. Furthermore, it was reported that the specimen collected on day 13 showed oseltamivir-resistant influenza A infection. Therefore, zanamivir instead of oseltamivir as well as ganciclovir were administered on day 23. The patient died of respiratory failure on day 27.

Case 2

A woman aged 66 years with asthma and chronic obstructive pulmonary disease (COPD) complained of fever (37.5 °C) and difficulty in breathing on September 12, 2009. A nasopharyngeal swab specimen was positive for influenza virus type A by the rapid diagnosis kit. The nasopharyngeal specimen was collected on September 15. The patient died of myocarditis on September 20, 2009.

Case 3

A woman aged 20 years complained of fever (38.2 °C) on November 26, 2009. A nasopharyngeal swab specimen collected on November 27 was positive for influenza virus type A by the rapid diagnosis kit.

Case 4

A girl aged 9 years complained of fever (37.0 °C) on December 9, 2009. Nasopharyngeal swab specimen [designated as Naso (pre) in Fig. 4] was negative for influenza virus type A by the rapid diagnosis kit. On the next day, a nasopharyngeal swab specimen [designated as Naso (after) in Fig. 4] was positive for influenza virus type A by the rapid diagnosis kit.

RNA extraction, RT-PCR, cloning, and sequencing

An autopsy of the patient of case 1 was immediately performed. About 1 g of tissue from the lower part of the lung was collected. Total RNA of the lung tissue was extracted using TRIAZOL by the manufacturer's instructions. Nasopharyngeal swab specimens from patients were subjected to RNA extraction with a QIAamp viral RNA kit (Qiagen, Hilden, Germany). Influenza virus genomic RNA was reverse transcribed using RT primer mixture (RT1: AGCAAAAGCAGGT; RT2: AGCGAAAGCAGGT; RT3: AGCAAAAGCAGGC; RT4: AGCGAAAGCAGGC; RT5: AGCAAAAGCAGGG; RT6: AGCGAAAGCAGGG), followed by the first polymerase chain reaction (PCR) using

NA/F primer ATGAATHCAAAHCADADDAT and the RT primer mixture. A second PCR was performed using NA/F primer and NA/R primer HHACTTGTCAATDGT DAATG. The amplicon fragment (1,411 bps) was extracted using GeneClean II (MP-Biomedicals, San Francisco, CA, USA). Sequence determination was outsourced to FASMAC, Kanagawa, Japan. The extracted amplicon fragment was ligated to pT7Blue-T vector (Novagen, Germany), and the recombinant plasmid was transformed into *Escherichia coli* (DH5α). The colonies were picked up and each NA sequence in the plasmid was determined as already described.

Sequence analysis

Parsimony-informative sites, which are parsimony informative in alignment of nucleic acid sequence if it contains at least two types of nucleic acids, and at least two of them occur with a minimum frequency of two, were extracted by the MEGA4 program [5] using all sequences determined by this study (Table 2). The proportion of nonsynonymous substitution (dN) and synonymous substitution (dS), and the ratio of dN to dS, were calculated using the SNAP program on the website (http://www.hiv.lanl.gov/content/sequence/SNAP/SNAP.html). A minimum spanning tree was constructed using the mst program of APE package in R software (R Development Core Team). In this program, each clone not only was mutually connected but also was plotted according to the parameters determined by additional nonsymmetrical correspondence analysis.

All sequences obtained in the present study have been submitted to GenBank under accession numbers HQ286390 to HQ286476.

Results

Intrahost variation of influenza virus under long-term oseltamivir treatment

The patient of case 1 was infected with the 2009 H1N1 virus and received oseltamivir (75 mg twice daily) for 21 days and zanamivir for another day (Table 1). He died of interstitial pneumonia on day 27 of his illness. We detected the H275Y mutation by direct sequencing from the nasopharyngeal samples on day 13 (Table 1) and confirmed it was resistant to oseltamivir [6]. The H275Y mutation was also detected in autopsy tissues from the right lung. In addition, we found a small but apparent signal of A (estimated 25 %) in the left lung (Fig. 1), indicating the presence of H257Y mutant population. To investigate the intrahost variation of influenza virus, RT-PCR products were cloned into a TA cloning vector and the NA gene from independent colonies was sequenced. The H275Y mutation was detected in all clones tested in 12 clones from the right lung and 11 clones from the nasopharynx (Table 2). However, the H275Y mutation was detected in 13 of 22 clones from the left lung. These results indicated that the H275Y mutant was the predominant population in both nasopharynx and right lung, whereas the H275Y mutant virus in the left lung was distributed with an equivalent population of oseltamivir-sensitive clones.

Intrahost evolution of H275Y mutant

To analyze the intrahost evolution of H275Y oseltamivir-resistant virus in case 1, we constructed a minimum spanning tree that provides a better understanding of sequence relationships for microevolution than standard phylogenetic tree representation [7]. Figure 2 shows the minimum spanning tree of all 45 clones from right lung, left lung, and nasopharynx. All H275Y mutants, except for the L7 clone, had additional common mutations at V80M and S82P, which were parsimony-informative sites (Table 2), suggesting that V80M and S82P might be important for the microevolution of oseltamivir-resistant virus. From the tree, the H275Y mutant was predicted to be derived from an oseltamivir-sensitive L2 clone, because the L2 clone was most closely related to the H275Y mutant and had common mutations at V80M and S82P. The L1 clone, in addition, was located to the center of all oseltamivir-sensitive clones. The L2 clone was supposed to be derived from L1, which is most similar to the putative origin of the Eurasian avian-like swine strain of pandemic influenza A (H1N1) 2009. The oseltamivir-resistant clone L7 was located in the same clade including oseltamivir-sensitive clones L6, L7, L8, L9, and L10 (Fig. 2), indicating that the L7 clone was originally derived from this oseltamivir-sensitive clade. The parsimony-informative amino acid of this L7 clone was the same as those of L1, except H275Y.

Intrahost variation of oseltamivir-sensitive virus in other cases

We further extended this approach to three other patients infected with the 2009 H1N1 influenza virus. Samples were taken from nasopharynx during acute phase before (cases 3 and 4) or after (case 2) oseltamivir administration. No H275Y mutant was detected in all 42 clones tested (Table 2). The clones were segregated into three major branches from the clone 33, which was most closely related to the putative origin of 2009 H1N1, European avian-like swine A/swine/Belgium/WVL1/1979 (Fig. 3). Clone 33 was also located between the L1 and L2 clones of case 1.

Table 2 Parsimony-informative sites of NA extracted by alignment of nucleotide sequences of all influenza virus clones determined by this study

Case	Region[a] and/or clone number	Position number of parsimony-informative site and assigned amino acid of clone 33											
		29 I	53 V	80[a] V	82[a] S	94 V	142 D	212 I	218 S	221 N	225 R	237 S	275[a] H	307 N
1	R1–R2			**M**	**P**								**Y**	
	R3			**M**	**P**	A							**Y**	
	R4–R5			**M**	**P**								**Y**	
	R6			**M**	**P**								**Y**	D
	R7			**M**	**P**					D			**Y**	
	R8		A	**M**	**P**								**Y**	
	R9–R11			**M**	**P**								**Y**	
	R12	R		**M**	**P**								**Y**	
	L1													
	L2			**M**	**P**									
	L3			**M**	**P**									
	L4		A											S
	L5										G			S
	L6													
	L7												**Y**	
	L8–L10													
	L11–L20			**M**	**P**								**Y**	
	L21			**M**	**P**							F	**Y**	
	L22			**M**	**P**								**Y**	
	N1–N8			**M**	**P**								**Y**	
	N9			**M**	**P**				G				**Y**	
	N10–N11			**M**	**P**								**Y**	
2	1–3								G					
	4											F		
	5–6													
	7						G							
	8–9													
	10						G	M						
	11													
3	12					A								
	13–14													
	15										K			
	16–21													
4	22	R						M						
	23		I											
	24							M		D				
	25–26							M						
	27			A				M						
	28							M						
	29							M		D				
	30–31							M						
	32–37													
	38										K			
	39–42													

[a] Key mutations are designated with bold font

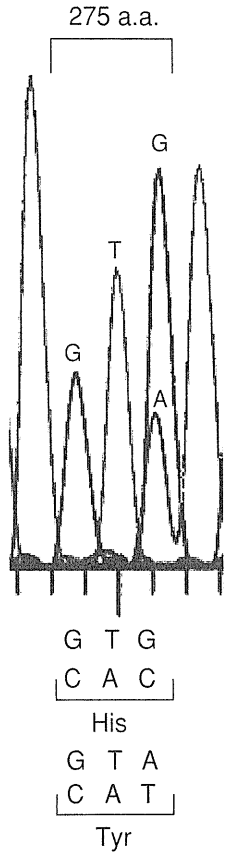

Fig. 1 Electropherogram of NA sequencing of the left lung virus around codon 275. The signal of each nucleotide is shown as the complementary. The first nucleotide G peak (*black*) at codon 275 overlapped with A peak (*green*) (color figure online)

We further compared the proportions of nonsynonymous substitution (dN) and synonymous substitution (dS) of all clones (Fig. 4). The proportion of dS of clones from left lung (case 1) was higher than that of other clones, which was ascribed to the tendency of the small dN/dS value of the left lung clones. The ratio of nonsynonymous substitutions (dN) and synonymous substitutions (dS) indicates positive selection (dN/dS >1) or purifying (stabilizing) selection (dN/dS <1). The dN/dS ratio of left lung clones (0.31 in Fig. 4) was the lowest in case 1, suggesting purifying selection preferentially contributed to the intrahost variation of left lung clones.

Discussion

Oseltamivir is a first-line treatment of patients infected with pandemic 2009 H1N1 virus, and the majority of 2009 H1N1 viruses remain susceptible to oseltamivir, although oseltamivir-resistant strains have been sporadically reported [3]. In this study, we first detected the H275Y mutation in the right lung but not in the left lung. There are few reports of the uneven distribution of oseltamivir-sensitive and oseltamivir-resistant viruses in a single patient [8]. Further analysis of intrahost variation of the virus in the left lung demonstrated that a part of the population was H275Y mutant and was predicted to be derived from oseltamivir-sensitive clone L1 (Fig. 2), which might be a descendant of

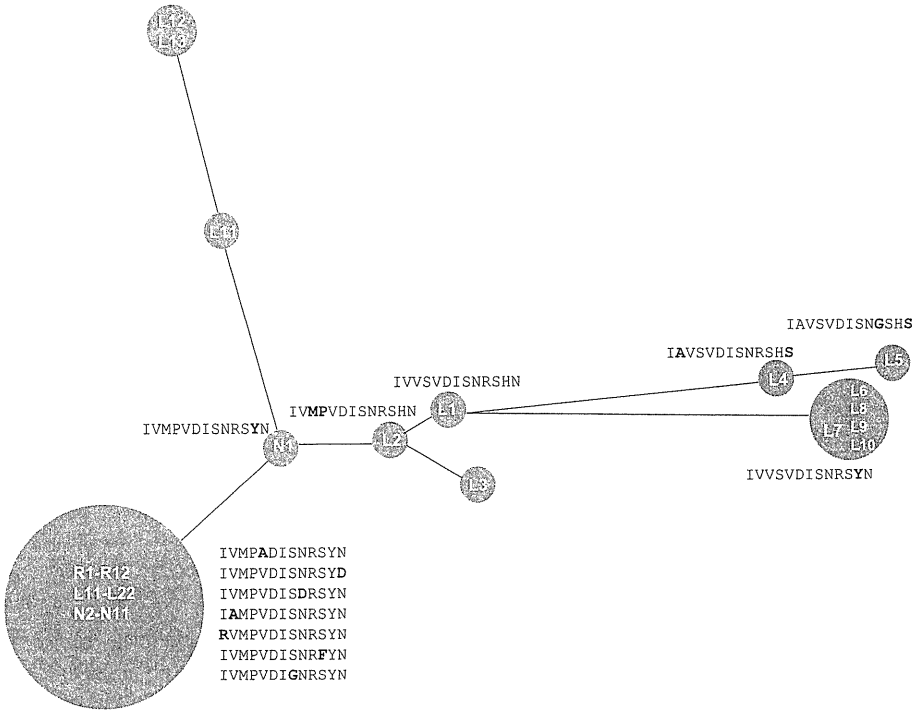

Fig. 2 Minimum spanning tree of intrahost variants of influenza virus in case 1. Eleven independent clones from the nasopharynx (*N1–N11*), 12 clones from the right lung (*R1–R12*), and 22 clones from the left lung (*L1–L22*) were used for constructing a tree and further arranged by two parameters derived from nonsymmetric correspondence analysis. Circle size is proportional to number of clones. Oseltamivir-sensitive clones and oseltamivir-resistant clones are shown in *blue* and *red*, respectively. A train of parsimony-informative amino acids extracted using all sequences from cases 1 to 4 is indicated beside each *circle*, and nonsynonymous mutations are shown in *bold* type. The train of clone L1 was set as the starting point for assessment of mutation (color figure online)

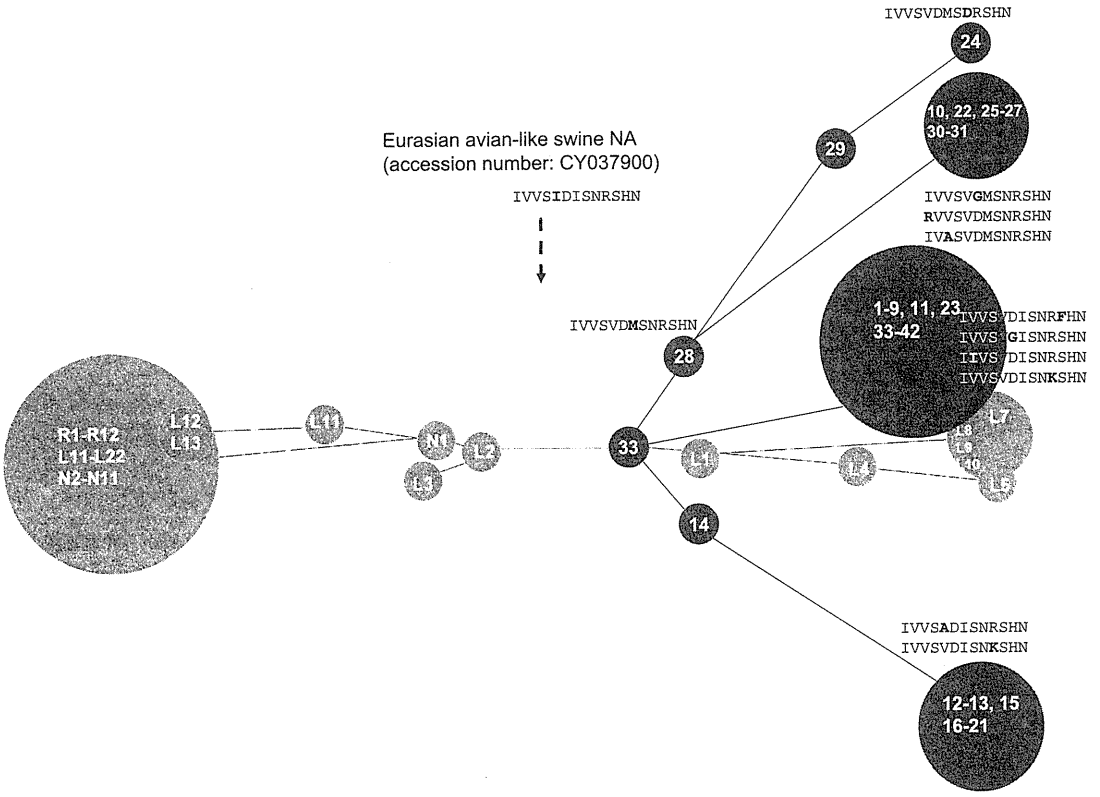

Fig. 3 Minimum spanning tree of intrahost variants of influenza virus in cases 2–4. Eleven independent clones from case 2 (*1–11*), 10 clones from case 3 (*12–21*), and 21 clones from case 4 (*22–31*, *32–42*) were analyzed as in Fig. 1. All specimens were taken from the nasopharynx. Oseltamivir-sensitive clones are shown in *blue*, and the tree was overlapped with that of case 1 (*faint color*). A train of parsimony-informative amino acids extracted using all sequences from cases 1 to 4 is indicated beside the *circles*, and nonsynonymous mutations are shown in *bold type*. The train of clone 33 was set as the starting point for the assessment for mutation (color figure online)

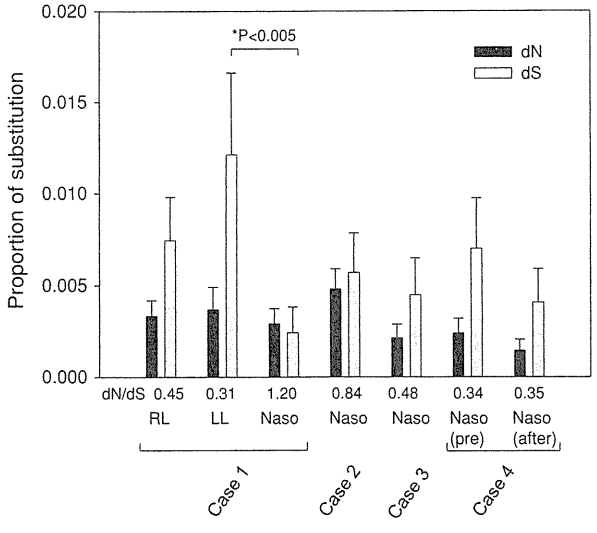

Fig. 4 Proportions of nonsynonymous substitution (dN) and synonymous substitutions (dS) of intrahost variants of influenza virus in cases 1 to 4. Data are shown as average ± SD. The dN/dS ratio is also shown. *Asterisk* indicates statistically significant by Student's *t* test. *RL* right lung, *LL* left lung, *Naso* nasopharynx

the putative oseltamivir-sensitive clone in the nasopharynx. Considering the route of virus spread from upper respiratory tract to lower respiratory tract, it is likely that the H275Y mutant is generated primarily in the nasopharynx, then spreads to the right and left lungs. In a study of other patients (cases 2–4), all intrahost species were oseltamivir sensitive, possibly because oseltamivir was administered briefly (case 2) or not administered at all (cases 3 and 4). Minimum spanning trees of all clones in this study determined clone 33, from the case 4 clones, as the core of oseltamivir-sensitive clones, indicating an origin of all intrahost species of oseltamivir-sensitive clones (Fig. 3). Interestingly, the oseltamivir-sensitive L1 clone of case 1 was also closely located to clone 33 and had common parsimony-informative amino acids (Table 2), which would predict a high degree of relatedness. In addition, clone 33 was most closely related to the putative origin of 2009 H1N1, European avian-like swineA/swine/Belgium/WVL1/1979. The dN/dS ratio of left lung clones from case 1 was smallest (Fig. 4). We also found a further decrease of the ratio of the oseltamivir-sensitive clone (dN/dS = 0.27), which was half of the population in the left lung, indicating

comparatively strong purifying selection occurred in the left lung [9]. It might be speculated that the oseltamivir-sensitive clone of the left lung is in a stable phase of evolution [9]. It is likely that case 1 might have been infected primarily with the oseltamivir-sensitive virus and that long-term administration of oseltamivir seems to have induced the generation of the H275Y mutant. Unfortunately, specimens were not available at the early phase of oseltamivir therapy, and we could not determine when the H275Y mutant was generated during therapy. Taken together, we supposed that the patient was infected with the L1 lineage first, which then spread to right and left lungs; it mutated independently in the left lung to L4–L10 strains but died out in the right lung (Fig. 2). In the nasopharynx, major clones having 80M, 82P, and 275Y appeared at about day 13 and spread to the right and left lungs at a later stage (Table 2). Thereafter, a small number of sensitive strains persisted stubbornly in the left lung although oseltamivir had been administered. It is still unclear, however, why the oseltamivir-sensitive clone still constituted half the total clones in the left lung despite the long-term administration of oseltamivir (21 days).

In summary, our study highlights the generation and intrahost variation of oseltamivir-resistant 2009 H1N1 virus under long-term oseltamivir therapy. This information allows us to predict the process of microevolution of an influenza virus within a host.

References

1. Smith GJ, Vijaykrishna D, Bahl J, Lycett SJ, Worobey M, Pybuset OG, et al. Origins and evolutionary genomics of the 2009 swine-origin H1N1 influenza A epidemic. Nature (Lond). 2009;459:1122–5.
2. Baranovich T, Saito R, Suzuki Y, Zaraket H, Dapat C, Caperig-Dapat I, et al. Emergence of H274Y oseltamivir-resistant A (H1N1) influenza viruses in Japan during the 2008–2009 season. J Clin Virol. 2010;47:23–8.
3. Campanini G, Piralla A, Rovida F, Puzelli S, Facchini M, Locatelli F, et al. First case in Italy of acquired resistance to oseltamivir in an immunocompromised patient with influenza A/H1N1v infection. J Clin Virol. 2010;48:220–2.
4. Hoelzer K, Murcia PR, Baillie GJ, Wood JL, Metzger SM, Osterrieder N, et al. Intrahost evolutionary dynamics of canine influenza virus in naive and partially immune dogs. J Virol. 2010;84:5329–35.
5. Tamura K, Dudley J, Nei M, Kumar S. MEGA4: molecular evolutionary genetics analysis (MEGA) software version 4.0. Mol Biol Evol. 2007;24:1596–9.
6. Ministry of Health: LaWoJ. Oseltamivir-resistant pandemic influenza virus in Kurume City. Press Release 26 February 2010.
7. Spada E, Sagliocca L, Sourdis J, Garbuglia AR, Poggi V, De Fusco C, et al. Use of the minimum spanning tree model for molecular epidemiological investigation of a nosocomial outbreak of hepatitis C virus infection. J Clin Microbiol. 2004;42:4230–6.
8. Furuse Y, Suzuki A, Kishi M, Nukiwa N, Shimizu M, Sawayama R, et al. Occurrence of mixed populations of influenza A viruses that can be maintained through transmission in a single host and potential for reassortment. J Clin Microbiol. 2010;48:369–74.
9. Kryazhimskiy S, Plotkin JB. The population genetics of dN/dS. PLoS Genet. 2008;4:e1000304.

J Infect Chemother (2012) 18:872–877
DOI 10.1007/s10156-012-0430-7

ORIGINAL ARTICLE

Use of high-dose IV and aerosolized colistin for the treatment of multidrug-resistant *Acinetobacter baumannii* ventilator-associated pneumonia: do we really need this treatment?

Gamze Kalin · Emine Alp · Ramazan Coskun · Hayati Demiraslan · Kürsat Gündogan · Mehmet Doganay

Received: 7 March 2012 / Accepted: 1 May 2012 / Published online: 29 May 2012

Abstract In this study we aimed to assess the safety and efficacy of high-dose IV colistin (COL) and aerosolized COL for the treatment of *Acinetobacter baumannii* ventilator-associated pneumonia (VAP). Critically ill adult patients who received IV COL for multidrug-resistant *A. baumannii* VAP were evaluated retrospectively. A total of 45 patients were evaluated [15 patients with high-dose COL (2.5 mg/kg every 6 h), 20 patients with normal dose (2.5 mg/kg every 12 h), and 10 patients with low dose, determined according to creatine clearance]. Aerosolized COL was used in 29 patients treated with parenteral COL and 16 patients received only parenteral COL. The clinical response rates on the fifth day were 50, 30, and 27 % with the normal, low, and high doses, respectively. However, the clinical response rates at the end of the therapy had declined to 30, 30, and 7 % with the normal, low, and high doses, respectively. The bacteriological clearance rates at the end of the therapy were 65, 75, and 64 %, with the normal, low, and high doses, respectively. With the aerosolized COL, the clinical response rates on the fifth day and at the end of the therapy were 35 and 14 %, whereas these rates were 44 and 38 % without the aerosolized COL. Bacteriological clearance rates with and without the aerosolized COL were 76 and 69 %, respectively. The nephrotoxicity rate was 40 % for the high-dose COL, whereas it was 35 % for the normal dose, and 20 % for the low-dose COL. In conclusion, higher doses of COL and aerosolized COL had no advantages over lower doses in alleviating multidrug-resistant *A. baumannii* VAP. Moreover, the higher doses and the aerosolized COL increased the nephrotoxicity risk and seemed not to be safe.

Keywords *Acinetobacter* spp. · Multidrug resistant · Colistin · Nephrotoxicity · Ventilator-associated pneumonia

Introduction

Ventilator-associated pneumonia (VAP) is a major safety problem in intensive-care units (ICUs) [1]. In recent years, the incidence of multidrug-resistant (MDR) *Acinetobacter baumannii* has been increasing, and the therapeutic options are limited [1, 2]. Colistin (COL; polymyxin E), an old class of antibiotic, was used for the treatment of infections with gram-negative microorganisms in the 1950s. It was abandoned in the 1980s because of its nephrotoxicity and neurotoxicity. However, after the emergence of MDR *A. baumannii*, COL was re-introduced for clinical use. However, the success rate of COL is questionable, with 25–70 % clinical effectiveness, and the optimal dose is controversial [3, 4].

The aim of this study was to investigate the safety and efficacy of different doses of IV COL (including a high dose) and aerosolized COL for the treatment of *A. baumannii* VAP.

Presented at the 4th Eurasia Congress of Infectious Diseases, 01–05 June 2011, Sarajevo, Bosnia and Herzegovina. Oral presentation 15.

G. Kalin · E. Alp (✉) · H. Demiraslan · M. Doganay
Department of Infectious Diseases and Clinical Microbiology, Faculty of Medicine, Erciyes University, 38039 Kayseri, Turkey
e-mail: ealp@erciyes.edu.tr

R. Coskun · K. Gündogan
Intensive Care Unit, Department of Internal Medicine, Faculty of Medicine, Erciyes University, Kayseri, Turkey

OPEN ACCESS Freely available online

PLoS one

The RNA Polymerase PB2 Subunit of Influenza A/HongKong/156/1997 (H5N1) Restrict the Replication of Reassortant Ribonucleoprotein Complexes

Yoko Nakazono, Koyu Hara*, Takahito Kashiwagi, Nobuyuki Hamada, Hiroshi Watanabe

Division of Infectious Diseases, Department of Infectious Medicine, Kurume University School of Medicine, Fukuoka, Japan

Abstract

Background: Genetic reassortment plays a critical role in the generation of pandemic strains of influenza virus. The influenza virus RNA polymerase, composed of PB1, PB2 and PA subunits, has been suggested to influence the efficiency of genetic reassortment. However, the role of the RNA polymerase in the genetic reassortment is not well understood.

Methodology/Principal Findings: Here, we reconstituted reassortant ribonucleoprotein (RNP) complexes, and demonstrated that the PB2 subunit of A/HongKong/156/1997 (H5N1) [HK PB2] dramatically reduced the synthesis of mRNA, cRNA and vRNA when introduced into the polymerase of other influenza strains of H1N1 or H3N2. The HK PB2 had no significant effect on the assembly of the polymerase trimeric complex, or on promoter binding activity or replication initiation activity in vitro. However, the HK PB2 was found to remarkably impair the accumulation of RNP. This impaired accumulation and activity of RNP was fully restored when four amino acids at position 108, 508, 524 and 627 of the HK PB2 were mutated.

Conclusions/Significance: Overall, we suggest that the PB2 subunit of influenza polymerase might play an important role for the replication of reassortant ribonucleoprotein complexes.

Citation: Nakazono Y, Hara K, Kashiwagi T, Hamada N, Watanabe H (2012) The RNA Polymerase PB2 Subunit of Influenza A/HongKong/156/1997 (H5N1) Restrict the Replication of Reassortant Ribonucleoprotein Complexes. PLoS ONE 7(2): e32634. doi:10.1371/journal.pone.0032634

Editor: Earl G. Brown, University of Ottawa, Canada

Received December 14, 2011; **Accepted** January 28, 2012; **Published** February 28, 2012

Funding: This study was supported by grants from the Ishibashi Foundation for the Promotion of Science and the Ministry of Education, Science, Sports and Culture, Japan, Grant-in-Aid for Young Scientists (B), 21791015, 2009–2010. The funders had no role in study design, data collection and analysis, decision to publish, or preparation of the manuscript.

Competing Interests: The authors have declared that no competing interests exist.

* E-mail: koyu@med.kurume-u.ac.jp

Introduction

Influenza A virus is a member of the family *Orthomyxoviridae*, and classified into subtypes by antigenic differences of the two surface glycoproteins, the hemagglutinin (HA) and the neuraminidase (NA) [1]. All 16 HA and 9 NA subtypes are maintained in aquatic birds and can be transmitted to various animals, including humans, pigs, horses and birds. However, avian influenza strains usually do not replicate efficiently in humans, and only three subtypes of H1N1, H2N2 and H3N2 have established sustained infection in human populations since the 1918 Spanish influenza, suggesting a significant restriction of transmission and adaptation of avian strains to humans.

The segmented genome structure of influenza virus facilitates genetic reassortment with other influenza strains which is co-infected in the same cells and has played a pivotal role in the emergence of pandemics. The pandemic strains of the past century have incorporated genes expressing the superficial HA and NA glycoproteins giving rise to new subtypes with novel surface antigens. Mutations of avian HA for acquiring human receptor α2, 6 sialic acid binding specificity is a prerequisite for human adaptation. In addition to acquiring novel genes for superficial glycoproteins, at least one internal gene of the RNA polymerase from avian strains has been concurrently incorporated into human strains. The1957 and 1968 influenza pandemics coincided with the introduction of an avian PB1 gene [2]. Similarly, the 2009 pandemic was caused by a reassortant that acquired PB2 and PA genes from an avian strain [3,4,5]. However, the contribution of polymerase genes to pandemic emergence has not been elucidated in detail.

The influenza virus RNA polymerase is a heterotrimeric complex composed of three subunits, PB1, PB2 and PA, which assembles with nucleoprotein (NP) and viral RNA, forming ribonucleoprotein complex (RNP) [6,7]. The PB1 subunit contains the S-D-D motif characteristic of polymerases and is directly involved in RNA synthesis [8,9]. The PB2 subunit binds to the cap structure at the 5′ end of host mRNA to generate short capped RNA fragments that are used as primers for viral transcription [6,10]. The PA subunit plays a role in transcription and replication through its endonuclease activity [11,12,13], promoter binding [13,14,15,16], cap binding [13] and possible proteolytic activity [17,18]. In addition to the central role of the RNA polymerase in RNA synthesis, recent studies have suggested its potential role in genetic reassortment [19,20,21,22]. Artificial hybrid RNA polymerases between human and avian influenza strains often exhibit a functional loss in RNA replication. Reconstitution experiments of influenza RNP in vivo has demonstrated that an introduction of avian PB2 into a background of human strains has often led to a

severe reduction of the polymerase activity [23,24]. It has also been suggested that a specific combination of avian PB2 with human PA or human PB1 leads to a significant decrease in polymerase activity [24,25]. However, the underlying mechanism that restricts genetic reassortment is still unclear.

In this study, we attempted to characterize and dissect the role of the polymerase genes in giving rise to a functional genetic reassortant. We generated RNP containing hybrid polymerase between human-isolated avian H5N1 and human H1N1 or H3N2. Our results revealed that the PB2 subunit of H5N1 has a strong inhibitory effect on the RNP activity when introduced into the polymerase of other influenza strains. Importantly, H5N1 PB2 could form functional 3P complex properly, but significantly reduced the accumulation of RNP, specifically through the properties of four amino acids in PB2 at position 108, 508, 524 and 627.

Materials and Methods

Strains

cDNA clones isolated from the following influenza strains were used: A/HongKong/156/1997 (H5N1) (abbreviated as HK or H), A/Vietnam/1194/2004 (H5N1) (abbreviated as VN or V), A/WSN/1933 (H1N1) (abbreviated as WSN or W), a newly pandemic A/Kurume/K0910/2009 (H1N1) (abbreviated as SW or S), A/NT/60/1968 (H3N2) (abbreviated as NT or N) [26].

Plasmids

PB1, PB2, PA and NP-expressing plasmids of influenza viruses HK, VN, WSN, SW and NT have previously been described [14,26,27]. The plasmid expressing vRNA of NA gene (vNA) from WSN has also been described previously [28]. Mutants of the PB2 plasmids were prepared by site-directed mutagenesis and were fully sequenced.

RNA isolation and primer extension assay in 293T cell

293T human embryonic kidney cells [12] were transfected with 0.2 μg each of PA, PB1, PB2, NP and vNA expression vector of each strain (WSN, NT, HK, VN or SW) by using Lipofectamine 2000 (Invitrogen). Cells were harvested 30 h posttransfection, and total RNA was isolated with TRIzol reagent (Invitrogen). RNA was then analyzed in a primer extension assay using three primers-one for vRNA, one for mRNA and cRNA, one for 5S rRNA as an internal control [12,13]. Transcripts were visualized by 7% polyacrylamide gel containing 7 M urea in TBE buffer and were detected by autoradiography. Assays were carried out at least three times with independently transfected cells.

Preparation of TAP-tagged polymerase and RNP and in vitro assays

For a preparation of the polymerase, 293T cells were transfected with expression vectors containing PB1, PB2 and TAP-tagged PA subunit of each strain. For a preparation of the RNP, NP and vNA expression vectors were also transfected simultaneously. Cells were harvested 2 days posttransfection and the polymerase or RNP was purified by the tandem affinity purification (TAP) method described previously [27]. Partially purified polymerase or RNP was analyzed by 7.5% SDS-PAGE with silver staining (Invitrogen) and confirmed by western blotting with specific antibody against PB1, PB2 and PA [17,29]. For in vitro assays, the amount of the polymerase was quantitatively adjusted. TAP purification procedure by PA TAP leads to co-purify trimeric complex with PB1-PA TAP heterodimer and PA TAP monomer, and the purified material reveals higher level of PA than other subunits. Adjustments were made by the quantitative measurements of the level of PB2 on silver-stained SDS-PAGE gel, because PB2 indicates the level of trimeric complex. The dinucleotide initiation of replication assay and UV cross-linking to model vRNA and cRNA promoters were performed as reported previously [16], and quantitated by autoradiography and Quantity One software version 4.6.7 (Bio-Rad).

Results

Effect of individual polymerase subunits of H5N1 on the RNP activity when reconstituted with other polymerase subunits of H1N1 or H3N2

In order to investigate the role of the RNA polymerase on the restriction of genetic reassortment, we reconstituted reassortant RNP by introducing the polymerase subunit of H5N1 into the polymerase of H1N1 or H3N2. We used two human-isolated H5N1 strains of A/HongKong/156/1997 [HK] and a closely related A/Vietnam/1194/04 [VN], two human H1N1 strains of A/WSN/33 [WSN] and the new pandemic influenza A/Kurume/K0910/09 [SW], and H3N2 strain of A/NT/60/68 [NT], because these strains were extensively analyzed previously [14,26]. The RNP was reconstituted in human 293T cells from hybrid polymerase on the background of WSN. The steady-state levels of NA reporter mRNA, vRNA and cRNA were measured by primer extension.

In the case of the HK strain of H5N1 (Figure 1, left 3 panels), the levels of mRNA, cRNA and vRNA were not significantly affected when HK PB1 alone, HK PA alone, HK PB1 - HK PB2 or HK PB1 - HK PA was introduced into WSN polymerase (Figure 1, lane 2, 4, 5 and 7). However, the RNP activity was severely reduced to essentially inactive levels, with only background levels of input vRNA, when either HK PB2 alone or HK PB2 - HK PA was introduced into WSN polymerase (Figure 1, lane 3 and 6). A similar significant reduction of RNP activities was also observed when either HK PB2 alone or HK PB2 - HK PB1 was introduced into SW (Figure 1, lanes 19 and 21) or NT polymerases (Figure 1, lanes 35 and 37). These results apparently showed that HK PB2 was responsible for the severe reduction of RNP activity, because HK PB2 alone could decrease the activity. This reduction of RNP activity was restored by HK PB1 in WSN polymerase (Figure 1, lane 5), or HK PA in SW or NT polymerase (Figure 1, lanes 22 and 38). On the other hand, in the case of the VN strain of H5N1 (Figure 1, right 3 panels), such remarkable reduction of RNP activity by the PB2 subunit was only observed when introduced into NT polymerase (Figure 1, lanes 43 and 45). VN PB2 did not show the inhibitory effect on either WSN or SW polymerases (Figure 1, lane 11, 14, 27 and 29). On the contrary, VN PB2 alone or VN PB2 - VN PB1 significantly increased the activity of SW polymerase (Figure 1, lanes, 27 and 29). These results indicate that the PB2 subunits of these two H5N1 strains differ in their properties when reconstituted into hybrid RNP with other influenza strains, and HK PB2 has a strong inhibitory effect on RNP activity.

Rescue of the hybrid RNP activity by mutations in HK PB2

Despite originating from the same H5N1 subtype, the amino acid sequence of PB2 between HK and VN differs at 26 positions out of 759 amino acids (Figure 2A). Since HK PB2 showed a severe reduction in RNP activity when introduced into other polymerases as compared to VN PB2, we speculated that a substitution of these 26 amino acids of HK PB2 for the VN PB2 sequence might rescue the impaired RNP activity. To test this,

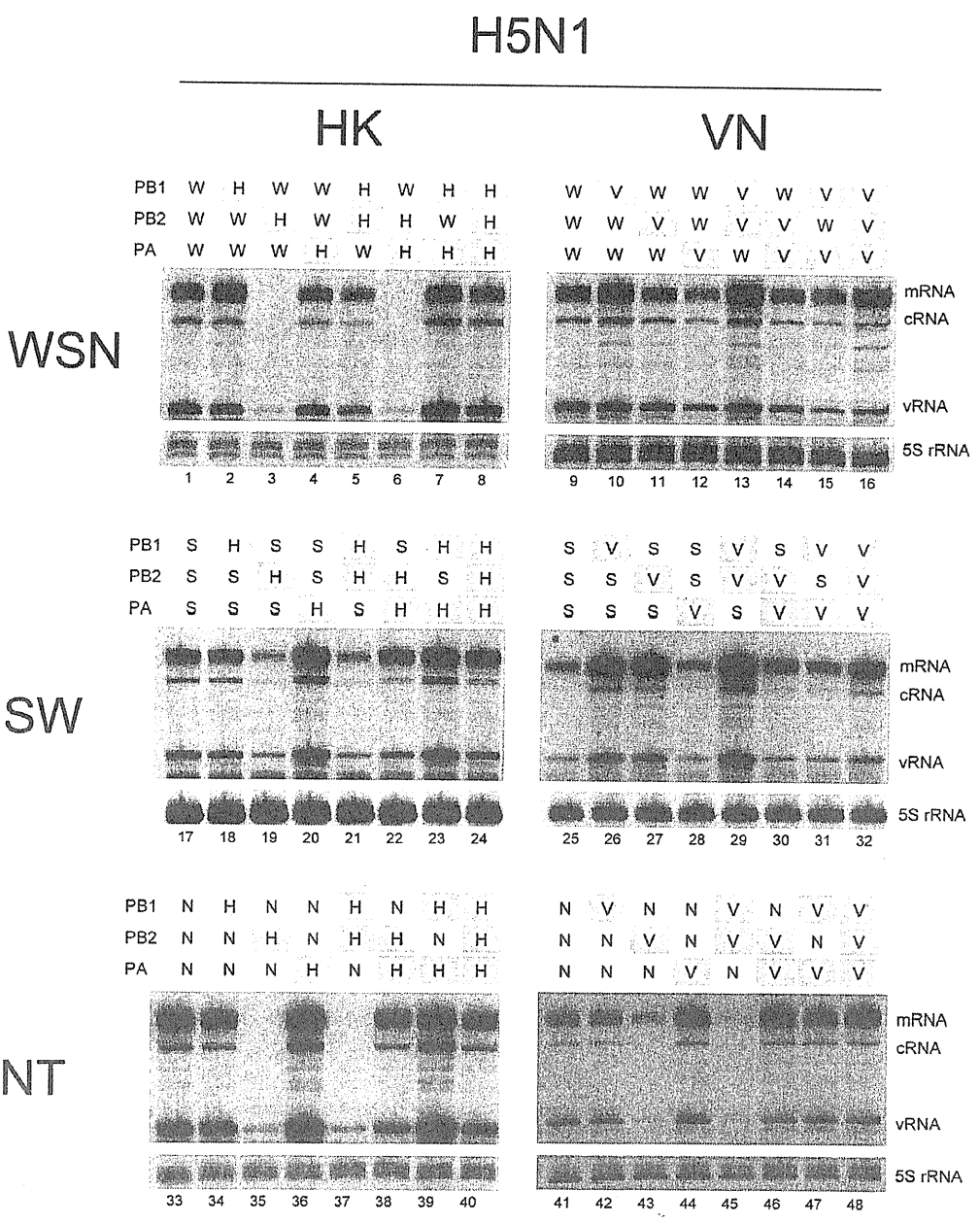

Figure 1. Comparison of RNP activities containing hybrid polymerases between H5N1 strains and human strains in vivo. Polymerase subunits of human strains of A/WSN/1933 (H1N1) (**W**), A/Kurume/K0910/2009 (H1N1) (S) and A/NT/60/1968 (H3N2) (N) were replaced with the corresponding subunits of A/HongKong/156/1997 (H5N1) (H) (left 3 panels) or A/Vietnam/1194/2004 (H5N1) (V) (right 3 panels). The RNP was reconstituted in 293T cells by transfection of plasmids expressing various combinations of polymerase subunits, and WSN derived NP and vNA. Total RNA was extracted 30 h posttransfection. Transcript products of viral mRNA, cRNA and vRNA were measured by primer extension and its positions are indicated on the right. The expected size of mRNA, cRNA, vRNA and 5S rRNA as an internal control are 169–177 nt, 160 nt, 129 nt and 100 nt, respectively.
doi:10.1371/journal.pone.0032634.g001

mutations were systemically introduced into HK PB2 at all positions, except for 4 residues at positions 190, 299, 340 and 355 because they were similar basic (R and K) amino acids. Firstly, we focused on residues 189 to 199 because amino acids differences between HK PB2 and VN PB2 were clustered in this region. However, all mutant polymerases K189E, K194Q, N195D, N197K and S199A showed still inactive levels of the RNP activity comparable to WT HK PB2 (Figure 2B, lanes 2 to 7). Next, we focused on residue 627 because PB2 K627 is known to be an important determinant for the virulence and host adaptation of influenza virus. A mutant polymerase E627K of HK PB2 rescued significant activity and the levels of all 3 RNA species (mRNA, cRNA and vRNA) reached about 50% of the VN PB2 activity (Figure 2B, compare lanes 17 with lane 10). In order to attempt to rescue RNP activity further, we then introduced additional mutations into the E627K mutant one by one. Mutations at C-

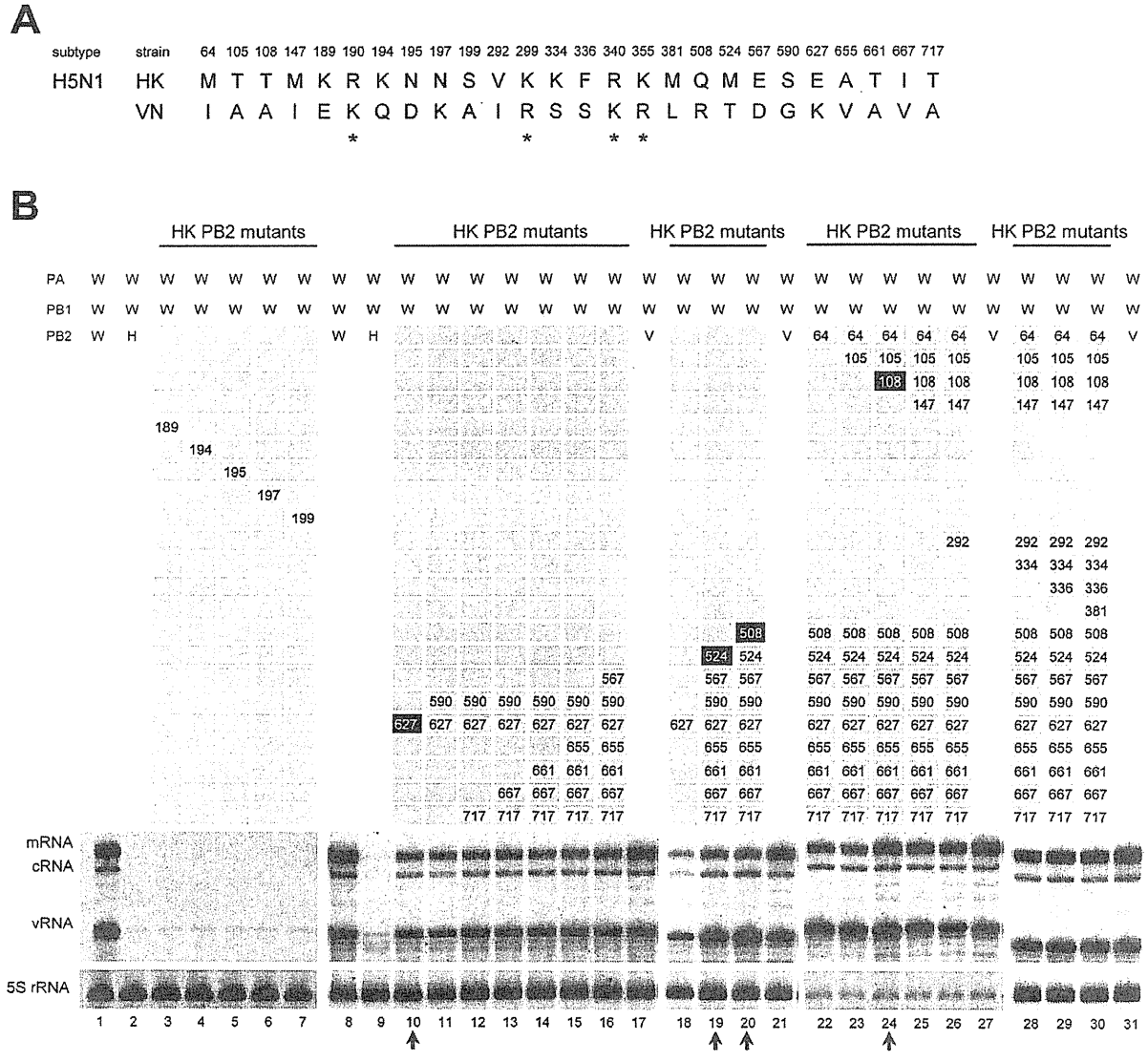

Figure 2. Effects of mutations in the HK PB2 subunit on the impaired RNP activity reconstituted from hybrid polymerase. (**A**) Alignment of amino acid residues of PB2 subunit differing between HK and VN of H5N1 strains. All positions of HK PB2, except for 4 residues (asterisk) that were similar basic amino acids, were sequentially substituted for VN PB2 sequences. (**B**) Steady state level of NA vRNA, mRNA, and cRNA in WSN (W) RNP reconstituted from hybrid polymerase by replacing only PB2 subunit with the HK PB2 wild type (H) (lanes 2 and 9), HK PB2 mutants (lanes 3–7, 10–16, 18–20, 22–26 and 28–30) and VN PB2 (V) (lanes 17, 21, 27 and 31). The numbers in HK PB2 mutants indicate mutated positions in HK PB2. Arrows indicate HK PB2 mutants which showed significant increase of RNP activity. The positions found to be important for the rescue of the RNP activity are highlighted.
doi:10.1371/journal.pone.0032634.g002

terminal regions did not further increase the RNP activity (Figure 2B, lanes 11–16). However, the additional mutation at M524T significantly increased activity, specifically of cRNA and vRNA, reaching the equivalent level to VN PB2 (Figure 2B, compare lanes 19 with 21). Subsequent mutation at Q508R further slightly increased vRNA to higher levels than VN PB2 (Figure 2B, lane 20), although the mRNA level was still lower than VN PB2. These results suggest a specific role of the positions 508 and 524 on the RNA replication (cRNA and vRNA synthesis), not on transcription (mRNA synthesis). The level of mRNA was fully rescued and the level of all three RNA species nearly reached the VN PB2 level when a mutation was subsequently introduced at T108A (Figure 2B, lane 24). Additional mutations did not increase the RNP activity further (Figure 2B, lanes 25–31). Overall, we conclude that at least 4 positions of 108, 508, 524 and 627 in HK PB2 are responsible for the impaired RNP activity reconstituted from hybrid polymerase.

Mutations at position 108, 508, 524 and 627 in VN PB2 impair the RNP activity

Since four amino acids in HK PB2 were found to be critical for rescuing activity of the hybrid RNP, it is conceivable that substitution of amino acids at the same position in VN PB2 by the HK PB2 sequence might decrease the RNP activity. Single

mutant R508Q or double mutant R508Q/T524M showed a slight decrease in activity compared with VN PB2 (Figure 3, lanes 3 and 4), while single mutant K627E showed a significant decrease in activity to less than 30% of mRNA, and ~10% of cRNA and vRNA (Figure 3, lane 5). The synthesis of all three RNA species was further decreased in a double mutant R508Q/K627 (Figure 3, lane 7), and markedly reduced to undetectable levels in a fourfold mutant A108T/R508Q/T524M/K627E (Figure 3, lane 9). Taken together, these results support our conclusion that 4 positions at 108, 508, 524 and 627 in HK PB2 are responsible for the optimal activity of RNP reconstituted from hybrid polymerase. We cannot exclude the possibility that residues other than 108, 508, 524 and 627 may also be important for RNP activity, because we have not tested HK PB2 carrying mutations at only these 4 positions.

HK PB2 impairs neither the assembly of trimeric complex nor the in vitro polymerase activity

To address the question why HK PB2 severely inhibited the activity of RNP reconstituted from hybrid polymerase, we initially examined whether HK PB2 affects the correct assembly of the trimeric complex of PB1, PB2, and PA. To allow the purification of trimeric complex, a C-terminally TAP-tagged PA was co-expressed with PB1 and PB2 in 293T cells, and the trimeric complex was affinity purified by a TAP method and quantitatively adjusted (see materials and methods). In the case of HK PB2, the expression level of three subunits was comparable to WSN polymerase or VN PB2 hybrid polymerase (Figure 4A, lane 2), although its RNP activity was impaired. A similar expression level of three subunits was observed in all four HK PB2 mutants having significant RNP activity (Figure 4A, lanes 3–6). Thus, HK PB2 does not appear to affect the correct assembly of the trimeric complex.

An alternative explanation for the defect of RNP activity is a loss of the polymerase activity. The binding of RNA polymerase to the promoter is an essential step to initiate RNA synthesis. Therefore, the promoter binding activity of the polymerase in vitro was assayed by UV cross-linking, then subsequent initiation of RNA synthesis was analyzed by dinucleotide replication assay (see materials and methods). Surprisingly, HK PB2 WT showed a strong activity to bind both vRNA and cRNA promoters (>200% of VN PB2 [Figure 4B and 4D, lane 2]), in spite of the loss of the RNP activity. However, the K627E mutation significantly reduced vRNA and cRNA promoter binding activities to the level of VN PB2 (100–150% of VN PB2 [Figure 4B and 4D, lane 3]). This suggests that position 627 might be involved in promoter binding. Additional mutations did not further affect promoter binding (Figure 4B and 4D, lanes 4–6). The promoter binding activity of the polymerase correlated well with the replication initiation activity and essentially similar results were observed. HK PB2 WT synthesized significant yields of ApG in both vRNA and cRNA templates (>200% of VN PB2 [Figure 4C and 4E, lane 2]). However, K627E mutation remarkably reduced the replication initiation activity (approximately 150% of VN PB2 [Figure 4C and 4E, lane 3]). Additional mutations had little effect on the activity (Figure 4C and 4E, lanes 4–6). Overall these results suggest that the impaired RNP activity by HK PB2 was not due to the defect in the assembly of the polymerase and the loss of the in vitro polymerase activity.

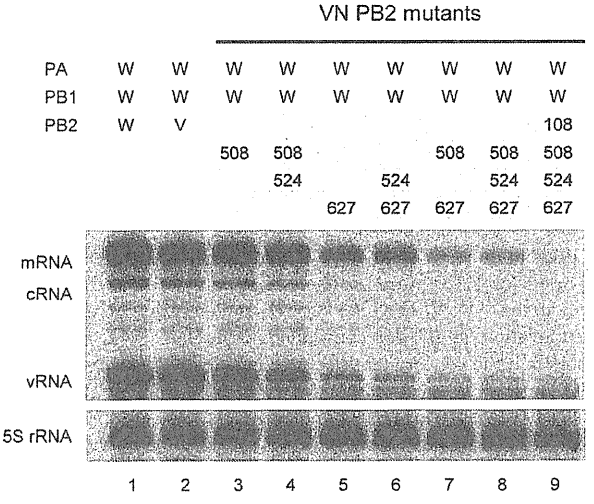

Figure 3. Effects of mutations in the VN PB2 subunit on the RNP activity reconstituted from hybrid polymerase. RNP of WSN (W) was reconstituted from hybrid polymerase by replacing only PB2 subunit with the VN PB2 wild type (V) (lane 2) or VN PB2 mutants (lanes 3–9). The steady state level of vRNA, mRNA, and cRNA was measured by primer extension. The numbers indicate mutated positions in VN PB2.
doi:10.1371/journal.pone.0032634.g003

HK PB2 impairs the accumulation of ribonucleoprotein complex

Another possible explanation for the loss of RNP activity is a defect in the assembly of RNP. To test this possibility, we purified and evaluated the amount of RNP accumulated in vivo. To allow RNP purification, a C-terminally TAP-tagged PA was coexpressed and the reconstituted RNP was affinity purified by a TAP method (see materials and methods). The amount of TAP-purified RNP was measured by Western blotting with specific antibodies for NP (Figure 5B and 5D). Addition of a C-terminal TAP tag at PA did not interfere with the RNP activity (data not shown). In the case of hybrid RNP containing VN PB2, NP was clearly detected, with an essentially similar level to that of WSN PB2 (Figure 5B and 5D, lanes 1 and 5). This indicates that the VN PB2 does not affect in vivo accumulation of RNP. By contrast, in the hybrid containing the HK PB2 (Figure 5A, lane 2) insignificant levels of RNP were detected (Figure 5B and 5D, lane 2), indicating the defect in the replication of RNP. Nevertheless the trimeric complex was correctly formed (Figure 5A, lane 2) and overall NP was expressed at equivalent levels to those seen in the wild-type WSN or VN (Figure 5C, lane 2 compared with lanes 1 and 5). These results clearly showed that HK PB2 had a major inhibitory effect on the accumulation of hybrid RNP. Importantly, the single mutation at 627 rescued significant accumulation of RNP, with an essentially similar level to that of VN PB2 (Figure 5B and 5D, lanes 3 and 5), suggesting that position 627 is obviously involved in the accumulation of RNP. However, the single mutation at 627 did not fully rescue the RNP activity and additional mutation at 108, 508 and 524 were required for the full activity (Figure 2). A significant level of RNP accumulation comparable to that of WSN PB2 or VN PB2 was also observed in the HK PB2 mutant with full RNP activity (Figure 5B and 5D, lane 4). Overall, these results suggested that HK PB2 significantly impairs the accumulation of RNP, explaining the loss of the RNP activity.

Discussion

The genetic reassortment between two different influenza A viruses can generate 256 (2^8) genotypes theoretically. However, systematic studies by using reverse genetics have shown that the number of replicative reassortant viruses is apparently limited

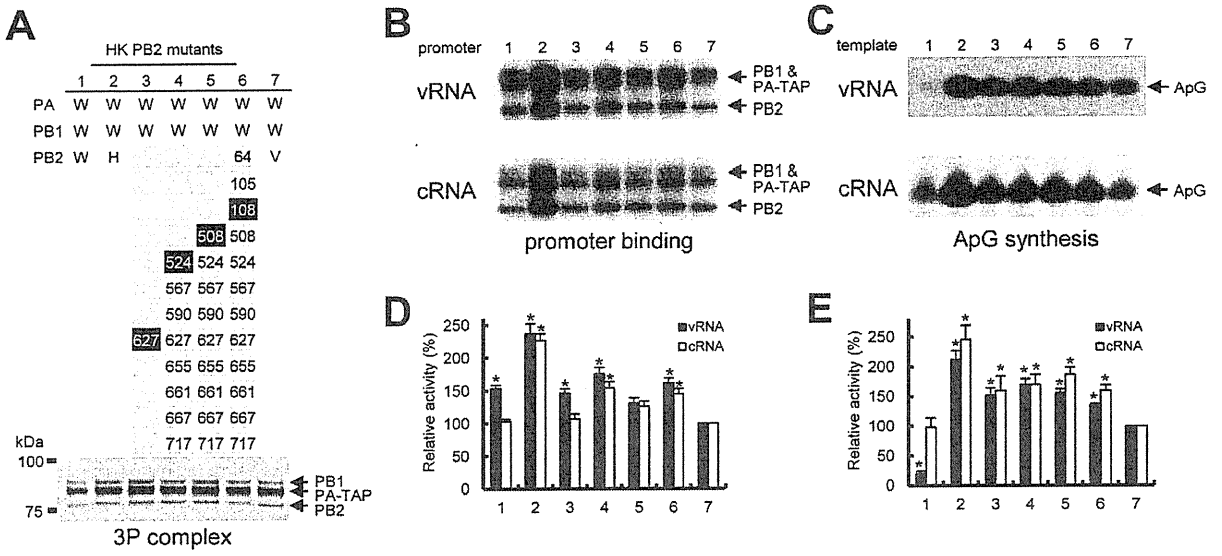

Figure 4. Promoter binding activity and replication initiation activity of HK PB2 mutants. (**A**) Partially purified polymerases analyzed by silver-stained 7.5% SDS-PAGE. Hybrid WSN (W) polymerase replaced only PB2 subunit with HK PB2 wild type (H) (lanes 2), HK PB2 mutants (lanes 3–6) and VN PB2 (V) (lane 7) was transiently expressed in 293T cells and partially purified by using TAP-tagged PA (see materials and methods). The numbers in HK PB2 mutants indicate mutated positions in HK PB2. The highlighted numbers are important for the rescue of the RNP activity. (**B**) UV cross-linking of model vRNA and cRNA promoters to hybrid polymerases. Purified and quantified polymerases were incubated with ^{32}P-labelled 3′ strand of the vRNA promoter in the presence of the unlabelled 5′ strand of the vRNA promoter (upper panel), or ^{32}P -labelled 3′ strand of the cRNA promoter in the presence of the unlabelled 5′ strand of the cRNA promoter (lower panel). Lane numbers correspond to the numbers in (A). The positions of the cross-linked products are indicated on the right. (**C**) ApG synthesis with a model vRNA promoter (upper panel) or cRNA promoter (lower panel). Lane numbers correspond to the numbers in (A). The position of the specific ApG product is indicated on the right. (**D and E**) Quantification of results obtained in panels B and C, respectively, by phosphorimaging. Data are expressed as percentages relative to VN PB2 (lane 7) (mean ± standard deviation; n = 3). Black bars, model vRNA promoter; white bars, model cRNA promoter. * shows statistical significance at $P<0.01$ in a Student's t-test.

doi:10.1371/journal.pone.0032634.g004

[23,25,30]. Reassortment between A/Thailand/16/04 (H5N1) and A/Wyoming/3/03 (H3N2), or A/equine/Prague/1/56 (H7N7) and A/Yokohama/2017/03 (H3N2), could yield only 63 (254 parent virus) or 29 (256 parent virus) hybrid genotypes, respectively [23,25]. In this study, we focused on the role of the RNA polymerase on the restriction of genetic reassortment of influenza virus. We constructed artificial hybrid RNPs by replacing the polymerase subunits of H1N1 or H3N2 with the corresponding subunits from two strains of H5N1, HK and VN, and evaluated the RNP activity by measuring steady state levels of mRNA, vRNA and cRNA. We found that the PB2 subunit of HK had a strong inhibitory effect on the activity both in transcription (mRNA synthesis) and replication (cRNA and vRNA synthesis), because it alone could inhibit the activity of all other strains (Figure 1). HK PB1 and HK PA did not appear to have this effect. These results are consistent with the observation that the PB2 subunit of avian or pandemic H1N1 has often lead to a reduction of activity in hybrid polymerase with human strains [23,24,31]. Interestingly, the pandemic human H2N2 and H3N2 does not carry avian PB2. Thus, we suggest that an introduction of the PB2 from certain avian H5N1 strains into human strains might be a disadvantage for successful genetic reassortment. Our results cannot exclude the possibility that NP may be involved, because other reassortment studies suggested the importance of NP in host adaptation [30,32,33,34].

Although few studies have described the mechanism of restriction of genetic reassortment, the loss of RNP activity in a hybrid experiment between equine H7N7 and human H3N2 strains was linked to the inability of assembly of the polymerase trimeric complex [25]. On the contrary, the polymerase trimeric complex was properly formed and no significant reduction of the in vitro polymerase activity was seen, even though the RNP activity was impaired when HK PB2 was introduced into the polymerase of other influenza strains (Figure 5). Our results clearly showed that the defect of RNP activity is related to poor accumulation of RNP. The RNP is formed by the association of vRNA to NP and polymerase trimeric complex. We can only speculate that HKPB2 may affect the efficiency of interactions of the polymerase with NP [35,36], vRNA and cellular factors [37,38] which are involved in the RNP assembly, thereby affecting RNP accumulation.

The correlation between the presence of lysine at position 627 of PB2 and the efficiency of RNP accumulation has recently been reported for H1N1 strains. The K→E mutation at PB2 627 of human strain A/WSN/1933 (H1N1) significantly decreased the accumulation of RNP reconstituted in human 293T cells and resulted in the concomitant decrease in the RNP activity [39]. In addition, the E→K mutation at PB2 627 of avian strain A/Mallard/Marquenterre/MZ237/1983 (H1N1) in 293T cells increased the accumulation of RNP [19]. These observations are in agreement with our data in H5N1 strains, indicating that the accumulation of RNP was almost fully rescued by the E→K mutation at 627. However, the single mutation at 627 could only partially rescue the RNP activity, and an additional mutation at 108, 508 and 524 was required for full recovery of the RNP activity (Figure 2). Thus, it is possible that amino acid at PB2 627 is mainly involved in the structural assembly of RNP, but other positions 108, 508 and 524 also play an important role in